Available online at www.sciencedirect.com
ScienceDirect
Colloids and Surfaces A: Physicochem. Eng. Aspects 300 (2007) 106–110
COLLOIDS AND SURFACES A
www.elsevier.com/locate/colsurfa

In silico study of the wettabilitty effects on gas cluster growth by solute diffusion in correlated porous media

C.M. Rodríguez [a], C. Felipe [b], A.M. Vidales [c], A. Domínguez [d,*], I. Kornhauser [d], F. Rojas [d]

[a] *Instituto Politécnico Nacional-ESIME Ticomán, Av. Ticomán No. 600, Col. San José Ticomán, 07340 Mexico City, Mexico*
[b] *Departamento de Fisicoquímica de Materiales, ICUAP, Benemérita Universidad Autónoma de Puebla, Puebla 72000, Mexico*
[c] *Depto. de Física, CONICET, Universidad Nacional de San Luis, 5700 San Luis, Argentina*
[d] *UAM-Iztapalapa, Departamento de Química, Av. San Rafael Atlixco 186, Col. Vicentina, 09340 Mexico City, Mexico*

Received 18 June 2006; received in revised form 12 October 2006; accepted 6 November 2006
Available online 17 November 2006

Abstract

Simulations of bubble growth in porous media are carried out with a 2D numerical automaton built on a set of hypotheses derived from experimental observations at pore scale. Various types of 2D numerical networks are used as models of porous media with the aim to study the outcome of the combined effects of the wettabilitty (homogeneous and mixed) and the spatial correlation among the porous network entities on the evolution of a gas cluster growing by solute diffusion into it. The porous networks are constructed by using a variation of the dual site bond model (DSBM) framework. For the same pore-size distribution, the DSBM can provide simulated porous media of different topological structures. Under these scenarios, numerical simulations concerning the growth pattern and the growth rate of a single gas cluster are performed.

Keywords: Automaton simulation; Bubble growth; Diffusion; Porous media; Spatial correlation; Wettabilitty

1. Introduction

Reservoir wettabilitty is a key parameter for oil recovery since it is accepted that during reservoir exploitation different wettabilitty scenarios can happen [1]. However, little is known about how reservoir wettabilitty can affect oil production during primary recovery. In this production interval, bubble growth by pressure drop of a gas-saturated liquid phase inside a porous medium plays a very important role [2]. It has been established that the laws of bubble growth inside porous media are very different from those followed in bulk [3,4]; the differences arise from the fact that the evolution of the gas–liquid interfacial area is strongly influenced by the porous medium microstructure. In this scenario, the interaction between the different variables is complex, and the use of numerical tools is useful for discerning the effects of the different variables ever since this helps in the interpretation of experimental results and allows the virtual exploration of the system evolution. In this work 2D simulations have been performed via a numerical automaton built under a set of hypotheses derived from experimental observations carried out at pore scale in 2D micro-models. This automaton has been tested through comparison between experimental and numerical results [4]. Now, it is used in order to carry out a systematic study on how the liquid–solid interactions and the characteristics of the spatial void distribution existing within a porous network can influence the evolution of a gas cluster growing by solute diffusion inside it. Diverse types of 2D numerical networks have been used as models of porous media; these were built by using a variant of the DSBM simulation framework [5,6]. For the same pore-size distribution, this pore network simulation provides media endowed with different bond-to-bond size correlation lengths, ξ_{BB}. This manuscript reports the results of such study.

2. Method

The method of research to be followed throughout this work can be divided in two main parts that involve:

(i) The construction of diverse types of numerical 2D square-lattice porous networks endowed with diverse degrees of

* Corresponding author. Tel.: +52 55 5 8044 762; fax: +52 55 5 8044 666.
E-mail address: doar@xanum.uam.mx (A. Domínguez).

0927-7757/$ – see front matter © 2006 Elsevier B.V. All rights reserved.
doi:10.1016/j.colsurfa.2006.11.020

spatial correlation among their void entities. The porous medium is represented by a 2D square lattice of sites joined through bonds (cf. [7]). All network elements are assumed to possess the same depth h. While sites are conceived as cylindrical disks with radius R_s, bonds have rectangular prism geometry with width $2R_b$; this bond shape allows the inclusion of solid wall roughness effects (liquid film) on bubble growth [8]. A similar network construction procedure has been previously described in a detailed manner in Ref. [5]. This procedure is based on a construction principle (CP) that establishes that the size of any site, R_s, should be larger than or at least equal to the size, R_b, of anyone of its connecting bonds, as well as on a parameter λ, which restricts the size differences existing among a pore and its neighboring void elements. The building procedure allows the construction of an assortment of auto-consistent networks, i.e. both CP and λ restrictions are fulfilled. The simulated networks have void elements belonging to the same pore-size distribution but which are spatially distributed in different ways. A characteristic feature caused by the restrictions imposed through this model is the formation of "patches" of sites and bonds having about the same sizes when the overlap between the site and bond size distributions is relatively high. The extent of these patches grows as correlations increase. The network is a 320×320 numerical matrix whose entries represent the sizes of the pore network constitutive elements (site, bond and solid, where the solid size is represented as 0). The sizes of bonds and sites are chosen from prearranged two-fold log-normal population samples. The statistical parameters of the bond-size distribution include a mean size $\bar{R}_B = 10^{-4}$ m and a standard deviation $\alpha = 1.5 \times 10^{-5}$ m; these values are chosen from [9]. In turn, for sites the mean size $\bar{R}_S$ is chosen as 1.1×10^{-4} m and α is assumed to be the same as that of the bond population. The lattice spacing distance is imposed to be equal to 18.9×10^{-4} m in order to simulate an experimental porosity value of 0.18 [9]. Therefore, the average length of the bond population is $\bar{l}_B = 16.7 \times 10^{-4}$ m. With respect to the affinity of the pore walls toward the fluids involved in the capillary process and although this is not be discussed here, there are physical reasons to consider that the largest pores can be preferentially considered as oil-wetted [5,10]. To investigate the way by which void elements are interconnected inside a simulated porous network, a bond-to-bond size correlation length, ξ_{BB}, is calculated by a Montecarlo method (at this respect cf. [7] and references therein). This quantity represents the mean extent (in lattice units) of patches where pore elements of similar sizes coexist.

(ii) The simulations of bubble growth in porous media by solute diffusion through a 2D numerical automaton, under different initial conditions (the process variables being the wettabilitty and ξ_{BB}). The automaton employed in this work is based on a pore modeling technique and a set of hypotheses derived from experimental observations made on 2D transparent micro-models [4]. Ref. [8] gives a full description of this automaton. The simulation assumes a porous network saturated with a liquid phase, under a uniformly distributed initial pressure P_0. Henry's law provides the initial uniform concentration of dissolved gas in the liquid phase as KP_0; K being Henry's constant. Next, an abrupt pressure drop ΔP is applied to the system and the generated gas super-saturation is good enough to induce the nucleation of one bubble in a given site, which is then quickly and fully occupied by gas; this stage can be considered as instantaneous. Next, the gas phase grows under the combined effects of solute diffusion and porous medium capillarity, while the liquid phase pressure, $P = P_0 - \Delta P$, is kept constant. Gas cluster growth is idealized as a succession of slow pressurization steps at constant gas cluster volume, and instantaneous stages of gas volume expansion at constant gas mass. Thus, the gas cluster growth rate can be conveniently computed through the duration of the pressurization periods, i.e. by knowing the time necessary for producing enough gas mass transfer into the bubble in order to create a critical pressure and to induce the movement of one or more menisci through neighboring bond-site pairs. The thermodynamic conditions used for the simulation purposes of this work are: $T = 293$ K, $P = 1$ bar and $\Delta P = 1.5$ bar; in particular the thermodynamic values of the system CO_2-*n*-decane studied in this work are: surface tension $\sigma = 23.43 \times 10^{-3}$ N/m, Henry's law constant $K = 4 \times 10^{-4}$ mol/(N m) and molecular diffusivity $D = 3.9 \times 10^{-9}$ m^2/s. The particular wettabilitty scenarios studied here are: (i) homogeneous wettabilitty, with contact angle $\theta \in \{0, \pi/6, \pi/3\}$, (ii) mixed wettabilitty, $\theta = 0$ for pores of size $< \bar{R}_s$ and $\theta = \pi/3$ for the biggest ones and (iii) mixed wettabilitty, $\theta = 0$ for pores with size $\geq \bar{R}_s$ and $\theta = \pi/3$ for the smallest ones. The output results of the program are: the gas cluster pattern, the time vector and the gas saturation vector. In the next section, these results are presented with the aim of showing the influences of the porous network's topology and of the liquid–solid interaction on the fluid phase distribution pattern and on the gas saturation, S_g, temporal evolution.

3. Results and discussion

Typical examples of results regarding the influence of ξ_{BB} on the pattern of a gas cluster are presented in Fig. 1, which shows the phase distribution of gas clusters occupying ~500 sites in three networks characterized by different ξ_{BB} values. According to Refs. [4,11] such visualizations show the classical characteristics of clusters generated by an invasion percolation algorithm, i.e. irregular shapes together with some trapping of the liquid phase. Note that the gas cluster shape changes from an irregular branched object to a dense disc, as ξ_{BB} increases. This is due to the gradual structuralization of the porous network as ξ_{BB} increases, i.e. a size-segregation effect progressively arises. This segregation effect means that regions of big pore entities that are linked together begin to appear and, in between them, there arise regions of smaller reunited pores [12]. Thus, the characteristic extension of pore zones is typified by a low (high) capillary energy increases throughout the porous network

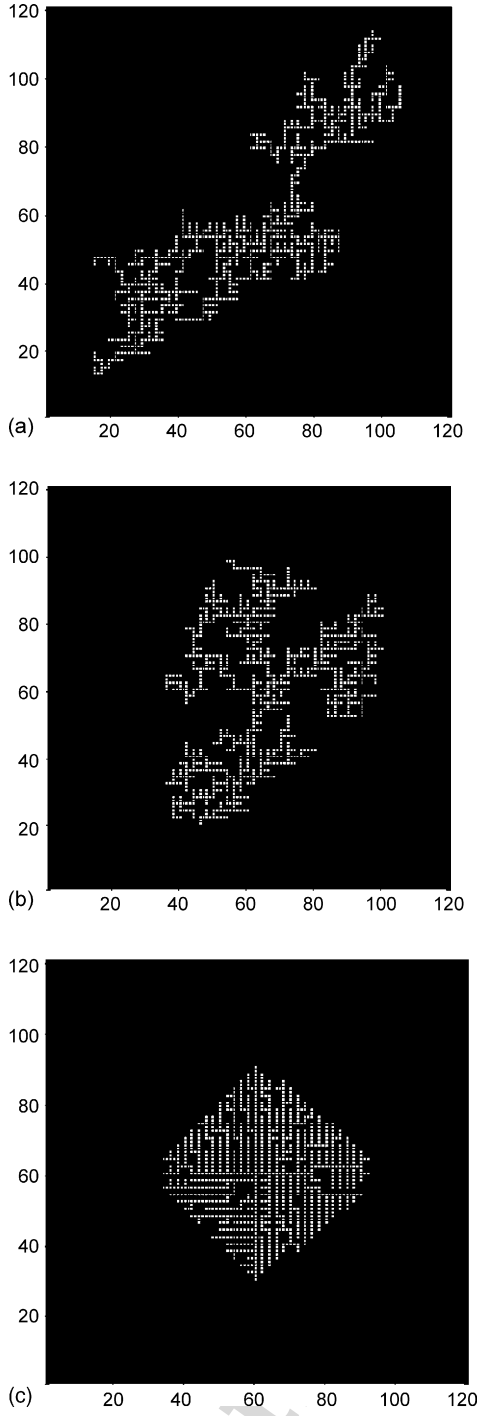

Fig. 1. Phase distribution of a gas cluster (white) occupying ~500 sites inside correlated porous networks. (a) $\xi_{BB} = 0.86 \pm 0.12$ and $D_f = 1.59 \pm 0.02$, (b) $\xi_{BB} = 4.53 \pm 0.12$ and $D_f = 1.66 \pm 0.02$ and (c) $\xi_{BB} = 10.63 \pm 0.12$ and $D_f = 1.75 \pm 0.02$. Homogeneous wettabilitty.

as ξ_{BB} gets larger (smaller). This fact modifies the fluid phase distribution since the gas phase grows seeking for the regions of the lowest capillary energy. The statistical ξ_{BB} error is estimated as 0.12. The gas cluster shape can be quantified via its fractal dimension, D_f (see, e.g. [13]), the statistical variability of this parameter is estimated as 0.02. Fig. 2 shows that while D_f varies from 1.59 ± 0.02 to 1.75 ± 0.02, ξ_{BB} changes from

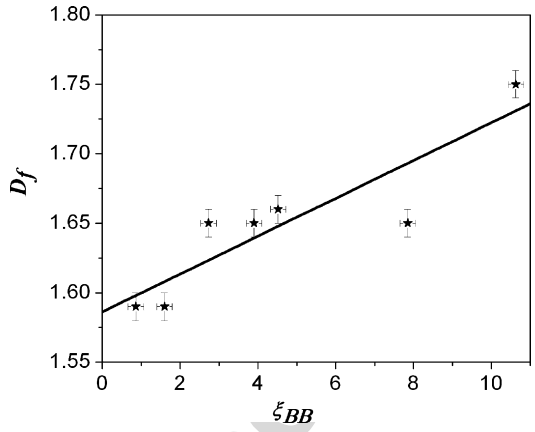

Fig. 2. Automaton simulation of correlated networks under homogeneous wettabilitty. The influence of ξ_{BB} on D_f. The best fit (continuous line) corresponds to: $D_f = 1.587 + 0.014\xi_{BB}$.

0.86 ± 0.12 to 10.63 ± 0.12, i.e. the gas phase fills the porous space more completely as ξ_{BB} becomes larger. Note the approximate linear relationship arising between them. The best data fit is represented by $D_f = 1.587 + 0.014\ \xi_{BB}$.

Concerning the S_g temporal evolution, it is pertinent to point out that, in the literature, the establishment of bubble growth laws in porous media is usually presupposed (see, e.g. [14]). For this reason, we have analyzed our results by means of the relationship $S_g \propto \tau^{\beta}$, where $\tau = Dt/\bar{l}_B^2$, t being the time of the gas-cluster growth. This kind of analysis has the advantage of clearly showing the effects of different variables on bubble growth [4]. The β exponent values are obtained from simulated S_g versus time curves. In all cases, it has been clearly observed the establishment of a definite growth law after performing the gas invasion of the first 200 sites; this being the reason why the β exponent is calculated from a set of 200 to 1000 gas-invaded sites. Fig. 3 shows the best fitting line (growth law) obtained from data proceeding from a specific numerical experiment. The β statistical error is 0.03. It is pertinent to point out that the network size effect is not considered as a variable due to the following reasons: (i) the gas cluster size is always very small with respect to the network that can hold as many as 25,600 sites and (ii)

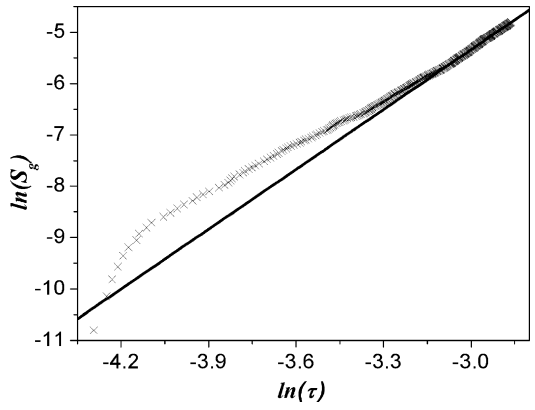

Fig. 3. Pore network simulation. $\ln(S_g)$ vs. $\ln(\tau)$ in order to observe the establishment of a growth law for $\tau > 0.04$. While crosses represent data from the simulator, the fitting line corresponds to the observed growth law.

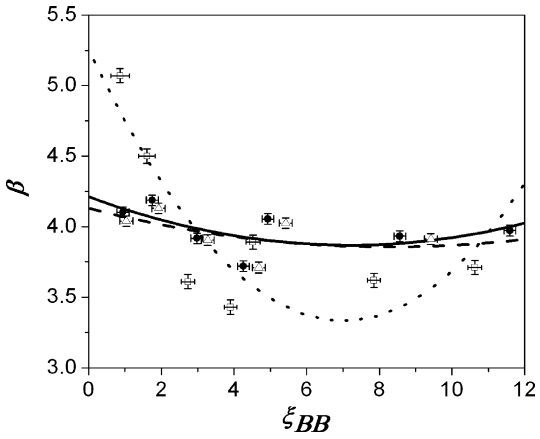

Fig. 4. Influence of ξ_{BB} on β under homogeneous wettabilitty conditions. Lines represent the best fits. (···) $\theta = 0$ and $\beta = 5.26 - 0.55\xi + 0.04\xi^2$; (—) $\theta = \pi/6$ and $\beta = 4.85 - 0.42\xi + 0.03\xi^2$; (- - -) $\theta = \pi/3$ and $\beta = 4.52 - 0.32\xi + 0.02\xi^2$.

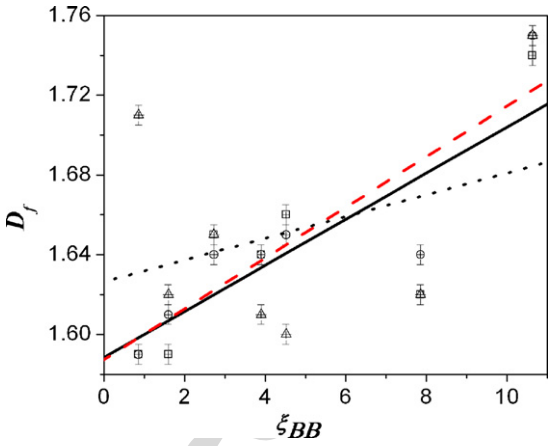

Fig. 5. Automaton simulation of correlated networks. Influence of ξ_{BB} on D_f under mixed wettabilitty conditions. (—) Ideal wetting, $D_f = 0.012\xi + 1.588$, (- - -) $\theta = 0$ for pores with size $\leq \bar{R}_s$ and $\theta = \pi/3$ for bigger ones, $D_f = 0.013\xi + 1.587$ and (···) $\theta = 0$ for pores with size $\geq \bar{R}_s$ and $\theta = \pi/3$ for smaller ones, $D_f = 0.005\xi + 1.626$.

we have taken care that the gas phase is not interacting with the network boundary, i.e. if the gas cluster touches the network border, then the corresponding virtual trial is discarded. Fig. 4 shows that, under a homogeneous wettabilitty situation, the volume (or S_g) of a single gas cluster tends to grow faster in porous media than in the bulk, i.e. a gas cluster grows via an exponent β greater than the values corresponding to the usual compact growth behavior displayed inside a homogeneous medium, $\beta = 1$ in 2D. Significant differences concerning β values, when ξ_{BB} increases from 0.86 ± 0.12 to 10.63 ± 0.12 are observed for $\theta \in \{0, \pi/6, \pi/3\}$. β values seem to be very sensitive to the evolution of the microstructure. First, β goes down as ξ_{BB} increases, however, this behavior changes for the highest ξ_{BB} values, since now β raises up. For the three cases under study, the plot β versus ξ_{BB} describes a parabolic trajectory. To explain this behavior, it is necessary to consider that the time required for menisci progression is controlled by both the gas mass transfer and the capillary constraint of the medium. If the mass transfer is improved or if the capillary constraint is decreased, then bubble growth is enhanced. Mass transfer depends on the solute concentration gradient around the gas cluster. Meniscus progression represents a partial renewal of the solute concentration gradient around the gas cluster; if a bond at the gas cluster boundary is drained of liquid then two or three additional super-saturated bonds are incorporated to the cluster boundary. From this perspective, ξ_{BB} hinders mass transfer since the area of influence of the gas cluster is reduced as ξ_{BB} grows, i.e. in lowly correlated networks the liquid–gas menisci progress towards gas super-saturated areas, while in highly correlated networks the liquid–gas interface evolves inside a relatively small area then producing the local annihilation of the gas super-saturation. On the other hand, with respect to capillary restrictions, in lowly correlated networks gas cluster borders are characterized by a more heterogeneous population of capillary thresholds due to a random repartition of network entities. In contrast to this behavior, pore-size structuralization in correlated networks overcomes the above random size repartition and the size-segregation effect allows a quicker cluster growth (i.e. a larger β value), since the mean capillary threshold in a higher correlated network is smaller than in a non-correlated one, thus improving bubble growth. As it can be seen in Fig. 4, the combination of these two effects produces a non-linear variation of β as function of ξ_{BB}. Data fitting renders the following relationships: $\beta = 5.26 - 0.55\ \xi_{BB} + 0.04\ \xi_{BB}^2$, $\beta = 4.85 - 0.42\ \xi_{BB} + 0.03\ \xi_{BB}^2$ and $\beta = 4.52 - 0.32\ \xi_{BB} + 0.02\ \xi_{BB}^2$ for θ equal to 0, $\pi/6$ and $\pi/3$, respectively. Notice that the curvature of the correlation $\beta = \beta(\xi_{BB})$ goes down as θ value increases since the capillary restrictions of the network tend to disappear as $\theta \to \pi/2$.

Mixed wettabilitty can magnify or reduce the capillary energy differences existing throughout the network; this kind of wettabilitty can have significant consequences over both, the gas cluster shape and the value of β. Results concerning the simulations of 2D bubble growth by solute diffusion in porous media expressed in terms of the cluster shape and the β values (as function of ξ_{BB}) and under the three wettabilitty scenarios are presented in Figs. 5 and 6. The explored wettabilitty scenar-

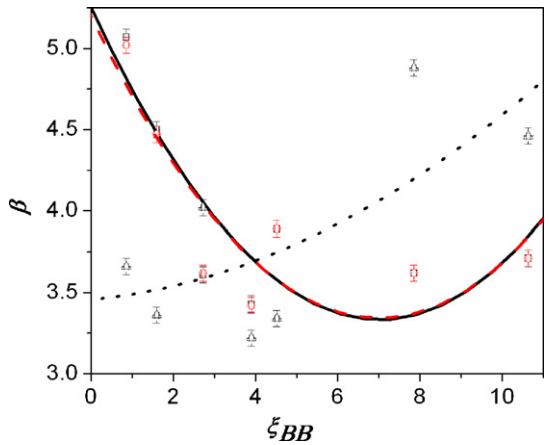

Fig. 6. Influence of ξ_{BB} on β under mixed wettabilitty regimes. Lines represent the best fits. (—) Ideal wetting, $\beta = 5.26 - 0.55\xi + 0.04\xi^2$, (- - -) $\theta = 0$ for pores with size $\leq \bar{R}_s$ and $\theta = \pi/3$ for bigger ones, $\beta = 5.20 - 0.53\xi + 0.04\xi^2$ and (···) $\theta = 0$ for pores with size $\geq \bar{R}_s$ and $\theta = \pi/3$ for smaller ones, $\beta = 3.46 - 0.02\xi + 0.01\xi^2$.

ios are: (i) ideal wetting, (ii) $\theta = 0$ for pores of size $< \bar{R}_s$ and $\theta = \pi/3$ for the biggest ones and (iii) $\theta = 0$ for pores of size $\geq \bar{R}_s$ and $\theta = \pi/3$ for the smallest ones. The two first wettabilitty situations produce very similar results regarding both, D_f and β versus ξ_{BB}, since in case (i), bubble growth occurs all the way through the largest pores and, in case (ii), the smallest pores are ideally wetted by the liquid phase, while the largest pores are only partially wetted by liquid; ideal wetting renders more difficult pore drainage, so the minima of capillary energy correspond again to the largest pores. Then in both cases, the gas–liquid interface progression occurs in the same way. On the other hand, case (iii) produces a different behavior for both, D_f and β versus ξ_{BB}. In this particular scenario, the largest pores are ideally wetted by the liquid phase, while the smallest pores are just partially wetted by liquid. Then, the drainage of small pores is now easier than in the two previous cases, and so the capillary energy minima are not only determined by the pore size; thus diminishing the influence of ξ_{BB}, i.e. the slope of the linear correlation $D_f = D_f(\xi_{BB})$ decreases, but also by the curvature of the parabolic decreasing behavior too. Thus, mixed wettabilitty can endorse the effects of ξ_{BB} when large pores are of a lyophobic nature, and can hold down ξ_{BB} effects when the largest pores are ideally wetted by the liquid phase.

4. Conclusions

This manuscript tries to provide new physical insights for the behavior of gas clusters growing inside porous media. A 2D numerical simulation was used in order to analyze the effects of various wettabilitty scenarios on bubble growth evolution inside correlated porous media; this kind of variable being very difficult to study experimentally. The numerical analysis developed here concerning the growing rate of an isolated single gas cluster, indicates that wettabilitty can exert a significant influence on both gas cluster growth and gas cluster morphology. For instance, ideal wetting can enhance the gas production kinetics if the porous network is weakly correlated, and when the liquid phase wets ideally the walls of the largest pores and only partially the walls of the smallest ones, this liquid–solid interaction hold down the effects of the spatial correlation existing among the pore network entities.

In spite of its limitations, the numerical tool employed in this work has been useful to study the influence of diverse parameters on gas cluster growth behavior. However, in order to continue with this study, some refinements are still required. For instance, it is known that a capillary process occurring inside a porous medium is strongly affected by the connectivity of the medium (cf. [12]). Connectivity promotes spatial size-segregation of pore elements; so the higher the connectivity, the more compact the gas cluster shape becomes. With respect to gas cluster growth kinetics, the balance of inhibitory (a narrow zone of influence) and promotive (low capillary constriction) effects should result in a non-linear relationship between connectivity and β. Quantitative verification of these likely trends is the goal of future work. In general, the study of the dimensionality effects can be integrated to the study of the connectivity effects when gravity is neglected. However, it would be interesting to develop a 3D version of the simulator, especially for situations in which gravity effects are important. A 3D version of the simulator is now being developed.

References

[1] F.A.L. Dullien, Porous Media: Fluid Transport and Pore Structure, first ed., Academic Press, New York, 1979, pp. 23–29.
[2] A. El Yousfi, C. Zarcone, S. Bories, R. Lenormand, Physical mechanisms for bubble growth during solution gas drive, SPE 38921 (1997) 805–809.
[3] X. Li, Y.C. Yortsos, Theory of multiple bubble growth in porous media by solute diffusion, Chem. Eng. Sci. 50 (1995) 1247–1254.
[4] A. Domínguez, S. Bories, M. Prat, Gas cluster growth by solute diffusion in porous media. Experiments and automaton simulation on pore network, IJMF 26 (2000) 1951–1979.
[5] A. Domínguez, H. Pérez-Aguilar, F. Rojas, I. Kornhauser, Mixed wettability: a numerical study of the consequences of porous media morphology, Colloid Surf. A 187/188 (2001) 415–424.
[6] S. Cordero, I. Kornhauser, A. Domínguez, C. Felipe, J.M. Esparza, F. Rojas, R.H. López, A.M. Vidales, J.L. Riccardo, G. Zgrablich, Review: site-bond modeling of disordered porous media, Part. Part. Syst. Char. 21 (2004) 101–116.
[7] C. Felipe, R.H. López, A.M. Vidales, A. Dominguez, 2D automaton simulation of bubble growth by solute diffusion in correlated porous media, Adsorption 11 (2005) 491–496.
[8] H. Pérez-Aguilar, A. Domínguez, C. Rodríguez, F. Rojas, I. Kornhauser, Virtual study of wettability effects on bubble growth by solute diffusion in correlated porous networks, Colloid Surf. A 206 (2002) 179–192.
[9] N.C. Wardlaw, J.P. Cassan, Oil recovery and the rock-pore properties of some sandstone reservoirs, Bull. Can. Petrol. Geol. 27 (1979) 117–138.
[10] A.B. Dixit, J.S. Buckley, S.R. McDougall, K.S. Sorbie, Empirical measures of wettability in porous media and the relationship between them derived from pore-scale modelling, Transport Porous Med. 40 (2000) 27–54.
[11] X. Li, Y.C. Yortsos, Visualization & simulation of bubble growth in pore networks, AIChE J. 41 (1995) 214–222.
[12] S. Cordero, F. Rojas, J.L. Riccardo, Simulation of three-dimensional porous networks, Colloid Surf. A 187/188 (2001) 425–438.
[13] A. Harrison, Fractals in Chemistry, Oxford University Press, New York, 1995, pp. 16–17.
[14] J.C. Moulu, Solution-gas drive: experiments and simulation, J. Petrol. Sci. Eng. 2 (1989) 379–386.